THE JOURNAL OF PHYSICAL CHEMISTRY C

Article

pubs.acs.org/JPCC

CO_2 Adsorption Sites in UTSA-16: Multitechnique Approach

Alessio Masala, Francesca Grifasi, Cesare Atzori, Jenny G. Vitillo, Lorenzo Mino, Francesca Bonino, Michele R. Chierotti, and Silvia Bordiga*

Department of Chemistry, NIS and INSTM Reference Centres, University of Torino, Via G. Quarello 15/A, 10135 and Via P. Giuria 7, 10125 Torino, Italy

Supporting Information

ABSTRACT: The key role of K^+ counterions in determining the high CO_2 capacity of UTSA-16 has been highlighted thanks to a combined use of in situ infrared and ^{13}C solid-state NMR spectroscopies performed in a controlled atmosphere at variable temperature and pressure. A second family of sites, engaged at higher temperature or at higher coverage, was identified in the organic linker. Variable temperature IR measurements of molecular hydrogen at 15 K allowed to further distinguish the K^+ sites in two families, slightly different in their polarizing ability and indistinguishable on the basis of CO_2 isosteric heat and by using a less sensitive probe than H_2, as CO and N_2.

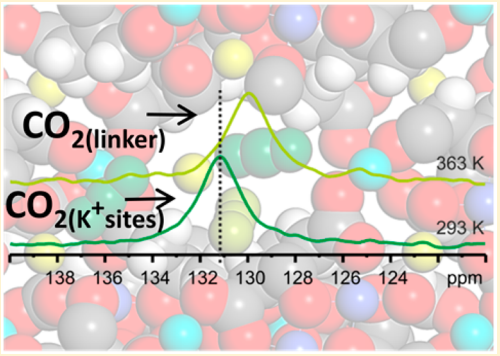

INTRODUCTION

Porous metal−organic frameworks (MOFs) are a well-known class of crystalline hybrid materials constituted of metal ions (isolated or clustered) bonded through rigid organic linkers that keep high microporosity once the solvent has been completely removed.[1] The tridimensional structure of these materials may be described on the basis of secondary building units (SBU) that characterize the metal cations and the organic linkers, both easily tunable to fulfill specific characteristics required to use them in technologic applications.[2−6] One of the most interesting properties of porous metal−organic frameworks is their high surface area as well as tunable pore size and pore volume. Thanks to these characteristics, MOFs have been extensively studied for small molecules capture, storage, and separation.[3,7−9] Within the extraordinary rich library of MOFs, Xiang et al.[10,11] introduced recently UTSA-16, showing its high performance as adsorbent for carbon dioxide, with a volumetric CO_2 uptake of 160 cm^3 cm^{-3} at 1 bar and 298 K.

Recently,[12] UTSA-16 ($K_2Co_3(cit)_2$, cit = $C_6H_4O_7$) was characterized by physical chemical techniques, suggesting as main CO_2 adsorption site, the K^+ counterions. Volumetric data of adsorbed CO_2 at 298 K and 1 bar (4.2 mol kg^{-1}) suggested that CO_2 not only saturates all the K^+ species present inside the UTSA-16 cavities forming 1:1 adducts, but that there was a consistent fraction of adsorbed CO_2 (approximately 22%) that exceeds and was characterized by an adsorption enthalpy almost coincident with that of the K^+ cations. The present work aims to highlight the nature of different adsorption sites in UTSA-16 combining solid state NMR of $^{13}CO_2$ and infrared spectroscopy using different probe molecules (H_2, N_2, and CO) thanks to measurements performed in controlled atmosphere at variable pressures and temperatures.

EXPERIMENTAL SECTION

UTSA-16 was prepared by SINTEF (Oslo-Norway) according to the synthesis described in literature.[10,11,13] Additional details are reported in section 1 of the Supporting Information. All chemicals were purchased by Sigma-Aldrich. Before any measurement, UTSA-16 was activated under high vacuum for 2 h and then heated up to 363 K overnight. Final vacuum was below 5×10^{-4} mbar. Carbon dioxide adsorption heat was measured at 303 K, with a Tian-Calvet microcalorimeter (Calvet C80, Setaram, France) connected to a grease-free high-vacuum gas-volumetric glass apparatus (residual p $\approx 10^{-4}$ mbar) equipped with a Ceramicell 0−100 mbar gauge (by Varian). In order to determine both integral heats evolved ($-q_{int}$) and adsorbed amounts (n_{ads}) a well established stepwise procedure was followed, described in section 2 of the Supporting Information.

Solid-state nuclear magnetic resonance (SSNMR) spectra were recorded on a Bruker Avance II 400 instrument operating at 400.23 and 100.65 MHz for ^1H and ^{13}C nuclei, respectively. Zirconia rotors (4 mm o.d., sample volume of 80 μL) were used. Additional details are given in section 3 of the Supporting Information.

CO_2 adsorption isotherms were measured at 273 and 298 K using a commercial volumetric instrument (TriStar II 3020 Micromeritics). The temperature stability was maintained by means of an isothermal water bath. In order to evaluate the isosteric heats of adsorption, CO_2 adsorption isotherms were fitted by a cubic spline function; each calorimetric point

Received: April 1, 2016
Revised: May 12, 2016
Published: May 13, 2016

ACS Publications © 2016 American Chemical Society

DOI: 10.1021/acs.jpcc.6b03333
J. Phys. Chem. C 2016, 120, 12068−12074

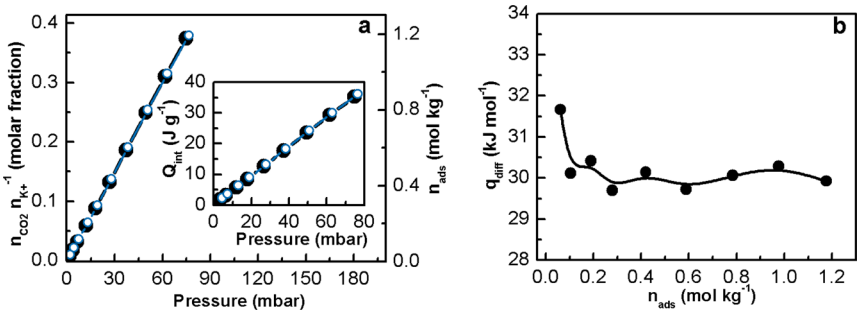

Figure 1. (a): Microcalorimetric first (black) and second (light blue, empty symbols) CO_2 volumetric isotherms (303 K) on UTSA-16. The CO_2 capacity is reported normalized to the number of K^+ ions (left of *y*-axis) and to the mass of the sample (right *y*-axis). The inset illustrates the variation of the integral heat of adsorption (Q_{int}) with respect to the pressure (calorimetric isotherm). (b): CO_2 differential heat of adsorption (q_{diff}) obtained from the data of primary CO_2 isotherm reported in (a).

reported in the inset of Figure 3 was obtained by applying the Clausius−Clapeyron equation defined as

$$q_{st} = RT^2\left(\frac{\partial \ln p}{\partial T}\right)_q \quad (1)$$

Plotting the natural logarithm of the pressure (p) as a function of $1/T$, a straight line (isosteric curve) was obtained whose slope is equal to $-q_{st}/R$ at constant loading (q): this is possible by assuming a Langmuir behavior of the adsorption and applying the Clausius−Clapeyron equation. The isosteric heat of adsorption is obtained by multiplying the slope by the perfect gas constant, as derived from eq 1.

For infrared (IR) measurements, UTSA-16 samples were prepared in form of self-supporting thin pellets. Before gas adsorption, samples were outgassed under high vacuum at 363 K overnight in the cryogenic cell (a closed circuit liquid helium Oxford CCC 1204 cryostat properly modified) allowing infrared investigation of species adsorbed under controlled temperature (between 300 and 15 K) and pressure conditions. Infrared spectra were recorded on a Bruker Equinox 55 FTIR spectrometer (sample compartment modified to accommodate the cryogenic head), 128 interferograms (1 cm^{-1} resolution) were averaged for each recorded spectrum. H_2 adsorption enthalpy was evaluated by variable temperature IR measurements, following the procedures described in literature[8,14] and explained in more details in section 4 of Supporting Information.

RESULTS AND DISCUSSION

CO_2 Adsorption by Microcalorimetry. Microcalorimetry was used to obtain a direct measure of CO_2 energetic interaction with UTSA-16 through the measurement of the heat of adsorption.

Figure 1a reports primary (black points and line) and secondary (light blue points and line) CO_2 adsorption isotherms obtained as described in section 2 of the Supporting Information. The adsorption profile suggests the presence of a single specific interaction site that is not saturated at the maximum coverage reached in the experiment (<100 mbar); moreover, the complete coincidence of the two isotherms indicates the total reversibility of the interaction of CO_2 with UTSA-16. In particular, the graph shows that less than 50% of the K^+ sites are interacting with CO_2 at this equilibrium pressure. Figure 1b illustrates the change in the differential heat of adsorption (q_{diff}) with increasing coverage for the primary adsorption of CO_2 (secondary adsorption is reported in Figure S1, Supporting Information); we note that the q_{diff} goes from 32 kJ mol^{-1} at 0.06 mol kg^{-1} to a constant value of 30 kJ mol^{-1}, over the full range of measurements, suggesting the presence of only one type of adsorption site, characterized by a medium interaction strength.[15] UTSA-16 CO_2 adsorption enthalpy is slightly higher than that reported for MOFs without exposed cations, as UiO-66 and UiO-66-NH_2 (22 and 27 kJ mol^{-1} respectively, see Table S1 in the Supporting Information).[16] For what concerns the comparison with MOFs having exposed cations, different factors determine the CO_2 adsorption enthalpy like charge/radius ratio, pore dimensions and shielding of the cation by the framework: for instance, the q_{diff} of UTSA-16 is similar to what reported for HKUST-1(Cu)[17] (28.2 kJ mol^{-1}) whereas it is slightly lower than that measured for MIL101(Cr)[3,18] (44 kJ mol^{-1}) and CPO-27(Mg)[19] (53 kJ mol^{-1}). In a previous paper,[12] reporting the isosteric heat of adsorption and IR data, it was shown that the most energetically favorable adsorption site was due to K^+ species, which are able to form 1:1 linear adducts with CO_2. The maximum capacity of the K^+ sites for CO_2 is 3.2 mol kg^{-1} for a 1:1 adduct. This indicates that for a CO_2 uptake higher than 3.2 mol kg^{-1} a second adsorption site must be involved. The interest in the nature of this second adsorption site relies in the fact that it is characterized by an adsorption enthalpy only slightly lower than the K^+ ion.[12]

As described below, NMR data allow to illustrate CO_2 adsorption features in a equilibrium pressure range not explored by microcalorimetry.

Solid State $^{13}CO_2$ NMR. SSNMR is an element-selective technique which can give new insights on the nature of adsorbed molecules and their interaction with the host surfaces, describing both CO_2 adsorption sites and CO_2 dynamics within the porous structure. Many SSNMR studies were conducted to investigate gas adsorption in zeolites, molecular sieves, or metal catalysts,[20,21] while only few of them were devoted to MOFs.[22−24]

$^{13}CO_2$ gas was dosed at different pressures (5, 20, 50, 100, 200, and 600 mbar) at 298 K on activated UTSA-16. A single signal, around 131 ppm, was observed at all CO_2 pressures (see Supporting Information Figure S2). Interestingly, the peak underwent a shift to lower frequencies (of about 1.1 ppm) on increasing the pressure, suggesting the presence of more than one CO_2 species within the MOF, thus more than one adsorption site inside the UTSA-16 cavities. For the samples at 200 and 600 mbar, variable temperature (VT) 293−373 K SSNMR measurements were also performed. These were instrumental to the detection and elucidation of exchange

DOI: 10.1021/acs.jpcc.6b03333
J. Phys. Chem. C 2016, 120, 12068−12074

phenomena among different molecular species of $^{13}CO_2$ within UTSA-16.

Figure 2 displays the ^{13}C MAS spectra of the sample at 200 mbar recorded at variable temperature (293 to 373 K). The

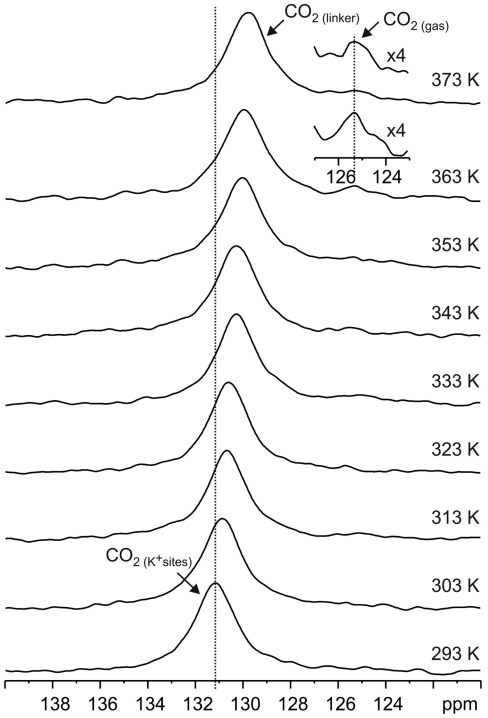

Figure 2. ^{13}C (100.65 MHz) MAS spectra with relevant assignments of $^{13}CO_2$-loaded UTSA-16 at 200 mbar in the temperature range from 293 to 373 K recorded with a spinning speed of 12 kHz.

spectrum at 293 K shows a single resonance at 131.2 ppm that can be ascribed to physisorbed CO_2. This signal shifts toward lower frequency on increasing the temperature. In the spectra at 363 and 373 K, in addition to the main contribution, now shifted to 129.7 ppm, a much weaker contribution at 125.3 ppm appears. The resonance peak at 125.3 ppm is easily assigned to the CO_2 in the gas phase (labeled as $CO_{2(gas)}$ in Figure 2), while the chemical shift of the main band (from 131.2 to 129.7 ppm) with increasing temperature reflects the dynamical behavior of adsorbed CO_2. Combining FTIR,[12] microcalorimetric, and SSNMR data, it was possible to assign the contribution at 131.2 ppm (clearly seen at coverage below 100 mbar at 293 K) to CO_2 directly interacting with K^+ (labeled as $CO_{2(K^+sites)}$ in Figure 2), while the signal at 129.7 ppm can be attributed to CO_2 still trapped inside the MOF cages and involved in a slightly weaker interaction probably with the organic linker (labeled as $CO_{2(linker)}$ in Figure 2), as indicated by the chemical shift with respect to $CO_{2\ (gas)}$.

Similar behaviors were already observed for CO and CO_2 loaded on $Cu_3(BTC)_2$: while the extent of the shift is comparable (~1.2 ppm), in those cases the resonance shift was toward lower frequencies.[25] This may be due to the difference in adsorption site (Cu vs K^+) and also to the difference in the metal component of the MOF (Cu vs Co with different paramagnetic character).

VT measurements were also performed on the sample with 600 mbar of CO_2 equilibrium pressure (see Supporting Information, Figure S3). In this case, the free CO_2 gas ($CO_{2\ (gas)}$) signal (125.3 ppm) becomes well visible at 333 K.

Dynamical data were derived from the chemical shift temperature dependence of the VT ^{13}C NMR spectra for adsorbed CO_2 molecules. The appearance of two distinct features at high temperature attributed, respectively, to CO_2 molecules in the gas phase ($CO_{2(gas)}$) and to those adsorbed in the MOF, indicating a slow exchange in the NMR time scale between adsorbed molecules and the gas phase under equilibrium conditions, without change of the total number of molecules. However, owing to the low signal intensity, the fraction of $CO_{2(gas)}$ cannot be estimated from the spectra,[25] so that it is not possible to obtain an enthalpy of activation for the exchange between these two CO_2 species. On the other hand, the temperature dependence of the signal related to CO_2 molecules adsorbed in the MOF reflected a fast exchange process, compared to that of the NMR time scale, between the strongly adsorbed molecules ($CO_{2(K^+sites)}$; $\delta \sim 131$ ppm) and those more weakly adsorbed ($CO_{2(linker)}$; $\delta \sim 130$ ppm). This observation leads to a determination of the exchange energy between $CO_{2(K^+sites)}$ and $CO_{2(linker)}$ by using eq 2 which allows the occupation number of the molecules adsorbed on K^+ sites to be calculated by considering the averaged shift due to the fast exchange between the molecules on K^+ sites and on the linker.

$$\delta(T)_{measured} = (1 - P_{(K^+sites)})\delta_{(linker)} + P_{(K^+sites)}\delta_{(K^+sites)} \quad (2)$$

$\delta_{(linker)}$ was extrapolated from the peak shift shown in Figure 2 to infinite temperature. In a similar way the measured low temperature values for $\delta_{(K^+sites)}$ were extrapolated with an error of 3 ppm. By using $P(T)_{adsorbed}$ and assuming an Arrhenius plot (see Supporting Information, Figure S4) a calorimetric quantification of the exchange phenomena between $CO_{2(K^+sites)}$ and $CO_{2(linker)}$ is then given by eq 2, from which an activation enthalpy of 6.3–9.3 kJ mol^{-1} (local motions in the MOFs; $CO_{2\ (K^+sites)} \leftrightarrow CO_{2\ (linker)}$) can be derived.

While magic angle spinning (MAS) spectra distinguished three types of CO_2 species, static spectra highlighted the dynamics of the processes through the analysis of the signal line shapes, as previously reported in the case of CO_2 adsorbed on Mg_2(dobdc).[18] The VT static ^{13}C NMR spectra are reported in Figure S5 (see Supporting Information). All spectra were characterized by a single very broad peak and no relevant changes were observed when the temperature was increased. The hump-like pattern of the static spectra (fwhm ~12 kHz compared to fast rotating $CO_{2(gas)}$, fwhm <1 kHz) provides direct evidence of a strong interaction between CO_2 and the MOF matrix. This implies a drastic reduction of the CO_2 motional freedom. Furthermore, the difference in line shapes from that typical of the CSA (chemical shift anisotropy) interaction suggests an intermediate motional regime of the $CO_{2(K^+sites)}$ on the binding sites characterized by disordered reorientational motion.[22−24]

Volumetric CO_2 Adsorption Measurements and Isosteric Heat of Adsorption. In order to validate the presence of a second adsorption site within UTSA-16, isosteric heat of CO_2 adsorption (Figure 3, inset) was calculated from the volumetric isotherms at 273 and 298 K until CO_2 loadings of 4.2 mol kg^{-1}, extending the pressure range described in a previous work.[12]

To briefly comment the isotherm curves which were widely discussed in our previous work,[12] it is possible to denote that the isotherm at 273 K reaches a maximum value (4.9 mol kg^{-1}) very close to the uptake calculated from the total volume of UTSA-16 pores, which was attested to 5.6 mol kg^{-1}.

DOI: 10.1021/acs.jpcc.6b03333
J. Phys. Chem. C 2016, 120, 12068−12074

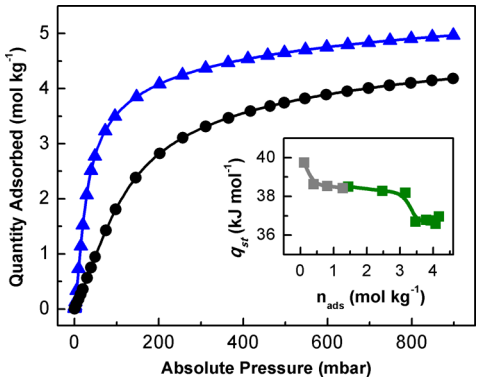

Figure 3. CO_2 volumetric isotherms on UTSA-16 at 273 (▲, blue points), and 298 K (●, black points) measured until 1 bar. Continuous lines represent the cubic spline fits computed on the experimental points. On the inset, the isosteric heat of CO_2 adsorption (■, green points) as a function of loading. The first five points of this trend (■, gray points) belong to ref 12 and they have been calculated with three isotherms at 273, 298, and 313 K.

In our previous work, a constant value (q_{st} = 38 kJ mol^{-1}) of CO_2 isosteric heat of adsorption (q_{st}) was calculated for a coverage range of 0.4−3.2 mol kg^{-1}, where the saturation of K^+ sites by carbon dioxide is not reached yet.[12] Reducing the number of isotherms involved in the calculation from three to two, it was possible to extend the coverage range well above the K^+ saturation point at 3.2 mol kg^{-1} and so to allow to estimate the isosteric heat associated with the adsorption of CO_2 over a second minor site, as shown in the inset of Figure 3: the first part of the trend below K^+ saturation is related to the interaction of CO_2 with K^+ sites as suggested by the isosteric heat value of 38 kJ mol^{-1} coinciding with the literature;[12,26] when the saturation of K^+ sites is reached, the isosteric curve steps down of 1 kJ mol^{-1} approaching an average value of 37 kJ mol^{-1}. This second constant trend confirms the results of NMR, indicating the presence of a second adsorption site other than K^+ cations. As already discussed in our previous work,[12] the isosteric heat of CO_2 adsorption calculated for UTSA-16 is one of the best among MOFs with exposed cations. Also when compared to MOFs with higher q_{st}, such as Mg_2(dobdc)[27] (47 kJ mol^{-1}) or Ni_2(dobdc)[28] (42 kJ mol^{-1}), the q_{st} of UTSA-16 does not drop down after saturation of the exposed cations. This can be related to the presence of tight pores (3.3 × 5.4 Å^2)[10] in UTSA-16 that promote the interaction of CO_2 with secondary adsorption sites other than potassium. An attempt to explain the nature of this site will be addressed by infrared spectroscopy.

VT-IR of Probe Molecules on UTSA-16. The nature of the second adsorption site in UTSA-16 was investigated by VT-IR spectroscopy by studying the adsorption of three probe molecules: H_2, N_2, and CO. Most relevant results are reported in Figure 4a−c.

VT-IR method allows to deduce, besides the information normally obtained from IR at constant T, the enthalpy of adsorption for very specific surface sites (see Supporting Information).[7,8,29]

Molecular hydrogen is one of the most attractive probe molecule for many reasons:[30,31] (i) the presence of a single bond between the two H−H atoms makes this molecule very sensitive to any surface heterogeneity, as even small perturbations originate shifts of the ν(HH), larger than those observed in case of probe molecules characterized by multiple

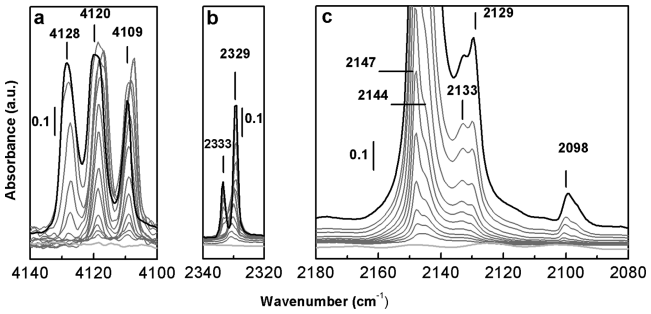

Figure 4. Background subtracted IR spectra of (a) H_2, (b) N_2, and (c) CO adsorbed on UTSA-16 at 15 K for H_2 and 60 K for N_2 or CO. Black lines correspond to the spectra collected in the presence of 0.1 mbar of H_2, 0.2 mbar of N_2, and CO equilibrium pressures, respectively. Light gray lines correspond to the spectra collected after outgassing overnight in a dynamic vacuum. Gray lines: intermediate coverage.

bonds (i.e., N_2 or CO); (ii) ν(H−H) mode is IR-inactive implying that every signal observed in the IR is related to the perturbations caused by the interaction of the probe with the surface sites; (iii) the small kinetic diameter (2.89 Å)[32] of this molecule allows to investigate in detail both cavities and surface active sites; and (iv) because of its amphoteric character, H_2 is able to test both acidic and basic surface sites.

A known amount of hydrogen (20 mbar) was dosed on the activated sample at 250 K and a series of spectra were collected while cooling until 15 K (1 spectrum each 5 K). The set of spectra recorded lowering the temperature are reported in the Supporting Information and were used to evaluate the adsorption enthalpy.

Figure 4a shows background subtracted spectra in the ν(H−H) region collected during outgassing at 15 K. For the sake of clarity we will describe the spectra starting from low to high coverage. At low equilibrium pressure, two main bands appear at 4109 and 4119 cm^{-1} and grow in parallel ($\Delta\nu$ = −52 and −42 cm^{-1}, respectively, in respect to ν-para-H_2 expected at 4161 cm^{-1}). Both values are compatible with the formation of side-on H_2 adducts with K^+ sites, on the basis of results reported for K-FER[33] or K-ZSM-5[34] ($\Delta\nu$ = −50 and −49 cm^{-1}, respectively) but in this case surprisingly sharp bands are observed (fwhm = 4 cm^{-1}). At higher coverage a further band appears at 4128 cm^{-1} ($\Delta\nu$ = −33 cm^{-1}) and becomes the most intense component at maximum H_2 loading (bold dark gray curve in Figure 4a). The last spectrum shows small changes in intensity ratio and maxima positions in respect to the medium coverage, suggesting that hydrogen, packing inside the small cavities of UTSA-16, undergoes some rearrangements in order to accommodate new incoming molecules. The frequency separation observed in case of the main doublet ($\Delta\nu$ = 11 cm^{-1}) is compatible with the co-presence of orto and para-H_2 but, in this case, upon decreasing the temperature, a change in the intensity ratio would have been expected after a waiting time of 15 h. In fact, it is known that para-H_2 (associated with the highest frequency component) is more stable at low temperature, with respect to the less stable orto-H_2 adduct.[8] Conversely, the intensity of the two peaks is constant since their appearance at 90 K (Figure S6a black line) also after a long waiting time. An alternative explanation can be given, implying the presence of two slightly different K^+—H_2 adducts arising from a difference in the orientation of H_2 (as already described in other MOFs),[7] or assuming two different K^+ sites

DOI: 10.1021/acs.jpcc.6b03333
J. Phys. Chem. C 2016, 120, 12068−12074

(K_1^+ and K_2^+). Finally, the peak at 4128 cm^{-1} is easily associated with H_2 perturbed by the oxygen atoms of the citrate organic linkers of UTSA-16, in line to what previously was observed in case of H_2 adsorbed inside microporous materials.[7,8,33,35] Thanks to the peak sharpness, an evaluation of H_2 adsorption enthalpy was obtained by the analysis of VT-IR spectra recorded in the 90 to 15 K temperature range. Following the procedure previously described[8,14] three values of H_2 adsorption enthalpy have been calculated (standard linear fits reported in Figure S7, S8, and S9 of the Supporting Information) and presented in Table 1. The presence of multiple interaction sites is in full agreement with what was suggested by $^{13}CO_2$ NMR measurements and CO_2 isosteric heat (see previous section). A graphic illustration of possible interaction sites for H_2 in UTSA-16 is shown in Figure 5.

Table 1. Summary of the Most Relevant Properties Obtained from VT-IR of Adsorbed H_2 for the Different UTSA-16 Active Sites[a]

UTSA-16	ν(H−H) (cm^{-1})	$-\Delta\nu$(H−H) (cm^{-1})	T_{onset} (K)	$-\Delta H_0$ (kJ mol^{-1})
K_1^+ site	4109	52	90	9 ± 1
K_2^+ site	4119	42	90	8 ± 1
linker site	4128	33	70	3 ± 1

[a] ν(H−H) indicates the frequency of H_2 vibration when interacting with the specific site; $-\Delta\nu$(H−H) indicates the red-shift from para-H_2 vibration (4161 cm^{-1}); T_{onset} is the highest temperature at which the signal first appears; $-\Delta H_0$ represent the enthalpy of H_2 adsorption for that precise site.

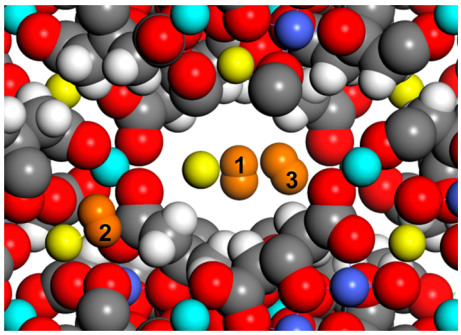

Figure 5. Structure of UTSA-16 as in refs 10 and 11 assuming the presence of extra-framework K^+ atoms (yellow, center of the pore). Water molecules and −OH groups have been omitted. The elements have been reported according to the following color code: carbon (gray), structural hydrogen (white), oxygen (red), cobalt (light blue for tetrahedral Co^{2+}, violet for octahedral Co^{2+}), potassium (yellow), and adsorbed hydrogen (orange). (1) H_2/K_1^+, (2) H_2/K_2^+, and (3) H_2/linker.

The stronger interaction between H_2 and UTSA-16 was detected, as expected, for the 1:1 adduction of H_2 with potassium with an enthalpy of adsorption of 9 kJ mol^{-1} for K_1^+ (T_{onset} = 90 K) and 8 kJ mol^{-1} for K_2^+ site. This value is in line with what obtained for K-ZSM5 by Otero Areán et al.[33] (8.9 kJ mol^{-1}) and slightly lower with respect to MOFs containing transition metals which show the highest H_2 enthalpy of adsorption up to 13 kJ mol^{-1}.[7,29]

The rearrangement seen in the IR spectra at higher loadings can be explained by a redistribution of the H_2 molecules which tend to condensate at higher coverage and low temperature.

The presence of an adsorption site related to the organic linker is definitely proven with H_2 and its signal is detected already at 70 K and 20 mbar of H_2 equilibrium pressure; the enthalpy of adsorption of this linker site is 3 kJ mol^{-1}.

A similar experiment was performed using N_2 as probe. N_2 vibrational mode, as for H_2, becomes IR active only after polarization by the surface. Because of the larger strength of the N≡N bond (945 vs 436 kJ mol^{-1} of H_2),[36,37] this molecule is less perturbed than H_2 after interaction with the surface. N_2 (40 mbar) was dosed on UTSA-16 at 150 K and then cooled down to 60 K, as shown in Figure S6b of the Supporting Information. The first spectrum was collected at 140 K and showed a maximum at 2330 cm^{-1}. At higher coverage (reached at lower temperature), two signals at 2329 and 2333 cm^{-1} grow at the expenses of the original band at 2330 cm^{-1}. The low intensity of all the components is due to the fact that the observed frequencies are only slightly shifted in respect to the unperturbed molecule (2321 cm^{-1} is the frequency observed in case of N_2 adsorbed at 240 K on silicalite).[38] Figure 4b reports the sequence of spectra collected upon lowering the nitrogen equilibrium pressure at 60 K. The two maxima at 2329 and 2333 cm^{-1} decrease in intensity and, at lower coverage, a single component at 2330 cm^{-1} is clearly visible. The evolution of the spectra suggests the formation of more than one adduct between K^+ species and N_2, with possible rearrangement of the local structure of the adducts. This could justify the appearance of a band associated with adsorbed N_2 at the highest frequencies (most perturbed) only at medium-high coverage.

Carbon monoxide is a probe largely employed for the characterization of different surface features such as alkaline metal cations, transition metal cations, or Lewis acidic centers.[31] It is commonly used to study microporous materials like zeolites with exchanged alkali-metals[39,40] or MOFs.[31,41−44]

CO was sent over UTSA-16 with an equilibrium pressure of 40 mbar at 60 K, that is a temperature lower than what is normally used for this kind of measurements (77 K),[31] in order to increase the coverage of this weak base and the number of active sites probed. Spectra reported in Figure 4c were plotted following the degassing of CO from the material. The single main band at 2147 cm^{-1} reassembles the formation of 1:1 adduct of CO with K^+ cation (K_1^+site), with the molecule attaching the site in end-on configuration; the corresponding band related to ^{13}CO is observed at 2098 cm^{-1}. Together with the signal at 2147 cm^{-1}, a red-shifted shoulder at 2144 cm^{-1} indicates the interaction of CO with a different K^+ site (K_2^+ site), as already seen by sending H_2 on the surface. At lower frequencies, a double peak is present: the signal at 2133 cm^{-1} is relative to the less typical interaction of CO with K_2^+ through the side of oxygen,[45] while the red-shifted component of this feature (2129 cm^{-1}) might be relative to CO interacting by the oxygen with a second K^+ (K_1^+ site). An alternative explanation to these bands can be postulated on the basis of the work reported by Otero Areán et al.[45] for CO adsorption in K-ZSM-5 who conceives the shoulder at 2144 cm^{-1} as due to the formation of a dual cation site complex where CO bridges two different K^+ sites. This bridging configuration of the CO molecule can take place only if the two adjacent K^+ sites lie at a distance of 7−9 Å.[46−48] No significant shift was noted while degassing CO from the material.

CONCLUSIONS

A detailed study on UTSA-16 metal−organic framework was performed by means of different physical-chemical techniques

DOI: 10.1021/acs.jpcc.6b03333
J. Phys. Chem. C 2016, 120, 12068−12074

to elucidate adsorptive properties toward small probe molecules. On our previous work,[12] the role of major active site in UTSA-16 was explained through the adsorption of CO_2, remarking a strong interaction toward K^+ cation present in the structure. Considering a formula unit such as $K_2Co_3(cit)_2$ (cit = $C_6H_4O_7$) and a pore volume of 0.32 $cm^3\ g^{-1}$, we estimated a saturation coverage for K^+ sites at 3.2 mol kg^{-1}. The isotherm at 298 K and 1 bar reported in ref 12 indicates a maximum CO_2 uptake of 4.2 mol kg^{-1}, 22% over the K^+ saturation limit. This fact points to the presence of another adsorption site other than potassium.

A multitechnique approach based on solid-state NMR, CO_2 isosteric heat evaluated until 1 bar, and the exploration of UTSA-16 surface by means of FTIR coupled with different probes allowed us to identify the presence of three adsorptions sites: two related to K^+ sites and one to the organic linker.

Microcalorimetric measurements quantified, in the low pressure range (below 100 mbar of equilibrium pressure), the presence of a single medium strength adsorption site (30.1 kJ mol^{-1}) assigned to CO_2 interacting with K^+ cations located inside the UTSA-16 channels. Conversely, solid-state NMR exploring a wider range of equilibrium pressure (to 600 mbar) was able to distinguish two different species of CO_2 molecules inside the MOF: $CO_{2(K^+site)}$ adsorbed on the K^+ adsorbing sites and $CO_{2(linker)}$ relative to a weaker interaction of CO_2 with the organic linker of the MOF. NMR results were in line with isosteric heat of CO_2 adsorption evaluated until 1 bar, that distinguished two families of sites with very close affinity for CO_2, 38 and 37 kJ mol^{-1}.

Moreover, the use of different small molecular probes coupled with IR spectroscopy shed light over the presence of two different adsorption sites, both related to K^+ sites. In particular, H_2 dosages at low temperature (15 K) allowed to identify two distinct K^+ species (labeled as K_1^+ and K_2^+sites) characterized by a H_2 adsorption enthalpy of 9 kJ mol^{-1} and 8 kJ mol^{-1}, respectively. Moreover, as already found in other MOFs, organic linkers represent a further adsorption site characterized by a lower interaction energy (3 kJ mol^{-1} in case of H_2). The existence of two distinct K^+ sites was also confirmed by IR data obtained in case of CO adsorption (maximum at 2147 cm^{-1}, associated with K_1^+ site and maximum at 2144 cm^{-1} to K_2^+ site).

■ ASSOCIATED CONTENT

Supporting Information

The Supporting Information is available free of charge on the ACS Publications website at DOI: 10.1021/acs.jpcc.6b03333.

Microcalorimetry (Figure S1); zero-coverage differential heat of CO_2 adsorption ($-\Delta H$) for some selected MOFs (Table S1); ^{13}C (100.65 MHz) SSNMR spectra of CO_2-loaded UTSA-16 at different equilibrium pressure or at different temperature recorded with a spinning speed of 12 kHz (Figure S2 and S3); dependence of $\ln(P_{(K^+sites)})$ on the reciprocal temperature (1000/K) for the sample at 200 mbar (Figure S4); ^{13}C (100.65 MHz) static spectra of $^{13}CO_2$-loaded UTSA-16 at 200 mbar in the temperature range from 293 to 353 K (Figure S5); VTIR spectra of H_2 and of N_2 adsorbed on UTSA-16 (Figure S6); van't Hoff plot (Figure S7, S8, and S9) (PDF)

■ AUTHOR INFORMATION

Corresponding Author

*E-mail: silvia.bordiga@unito.it; Tel:0039 011 6708373.

Notes

The authors declare no competing financial interest.

■ ACKNOWLEDGMENTS

The research leading to these results has received funding from the European Union Seventh Framework Programme (FP72007−2013) under Grant Agreement 608534 (MATESA project). We also would like to acknowledge Dr. Carlos Grande and the SINTEF group for providing UTSA-16 MOF.

■ REFERENCES

(1) Yaghi, O. M.; O'Keeffe, M.; Ockwig, N. W.; Chae, H. K.; Eddaoudi, M.; Kim, J. Reticular Synthesis and the Design of New Materials. *Nature* **2003**, *423*, 705−714.

(2) Furukawa, H.; Cordova, K. E.; O'Keeffe, M.; Yaghi, O. M. The Chemistry and Applications of Metal-Organic Frameworks. *Science* **2013**, *341*, 974−986.

(3) Sumida, K.; Rogow, D. L.; Mason, J. A.; McDonald, T. M.; Bloch, E. D.; Herm, Z. R.; Bae, T. H.; Long, J. R. Carbon Dioxide Capture in Metal-Organic Frameworks. *Chem. Rev.* **2012**, *112*, 724−781.

(4) Vitillo, J. G. Magnesium-Based Systems for Carbon Dioxide Capture, Storage and Recycling: From Leaves to Synthetic Nanostructured Materials. *RSC Adv.* **2015**, *5*, 36192−36239.

(5) Furukawa, H.; Ko, N.; Go, Y. B.; Aratani, N.; Choi, S. B.; Choi, E.; Yazaydin, A. O.; Snurr, R. Q.; O'Keeffe, M.; Kim, J.; et al. Ultrahigh Porosity in Metal-Organic Frameworks. *Science* **2010**, *329*, 424−428.

(6) Deng, H. X.; Grunder, S.; Cordova, K. E.; Valente, C.; Furukawa, H.; Hmadeh, M.; Gandara, F.; Whalley, A. C.; Liu, Z.; Asahina, S.; et al. Large-Pore Apertures in a Series of Metal-Organic Frameworks. *Science* **2012**, *336*, 1018−1023.

(7) Vitillo, J. G.; Regli, L.; Chavan, S.; Ricchiardi, G.; Spoto, G.; Dietzel, P. D. C.; Bordiga, S.; Zecchina, A. Role of Exposed Metal Sites in Hydrogen Storage in MOFs. *J. Am. Chem. Soc.* **2008**, *130*, 8386−8396.

(8) Chavan, S. M.; Zavorotynska, O.; Lamberti, C.; Bordiga, S. H2 Interaction with Divalent Cations in Isostructural MOFs: A Key Study for Variable Temperature Infrared Spectroscopy. *Dalton Trans.* **2013**, *42*, 12586−12595.

(9) Fracaroli, A. M.; Furukawa, H.; Suzuki, M.; Dodd, M.; Okajima, S.; Gandara, F.; Reimer, J. A.; Yaghi, O. M. Metal-Organic Frameworks with Precisely Designed Interior for Carbon Dioxide Capture in the Presence of Water. *J. Am. Chem. Soc.* **2014**, *136*, 8863−8866.

(10) Xiang, S. C.; He, Y. B.; Zhang, Z. J.; Wu, H.; Zhou, W.; Krishna, R.; Chen, B. L. Microporous Metal-Organic Framework with Potential for Carbon Dioxide Capture at Ambient Conditions. *Nat. Commun.* **2012**, *3*, 954−962.

(11) Xiang, S. C.; Wu, X. T.; Zhang, J. J.; Fu, R. B.; Hu, S. M.; Zhang, X. D. A 3D Canted Antiferromagnetic Porous Metal-Organic Framework with Anatase Topology through Assembly of an Analogue of Polyoxometalate. *J. Am. Chem. Soc.* **2005**, *127*, 16352−16353.

(12) Masala, A.; Vitillo, J. G.; Bonino, F.; Manzoli, M.; Grande, C. A.; Bordiga, S. New Insights into UTSA-16. *Phys. Chem. Chem. Phys.* **2016**, *18*, 220−227.

(13) Grande, C. A.; Agueda, V. I.; Spjelkavik, A.; Blom, R. An Efficient Recipe for Formulation of Metal-Organic Frameworks. *Chem. Eng. Sci.* **2015**, *124*, 154−158.

(14) Bonino, F.; Lamberti, C.; Chavan, S.; Vitillo, J. G.; Bordiga, S. Characterization of MOFs. In *Metal Organic Frameworks as Heterogeneous Catalysts*; Xamena, F., Gascon, J., Eds.; Royal Soc Chemistry: Cambridge, 2013; pp 76−142.

(15) Bolis, V. Fundamentals in Adsorption at the Solid-Gas Interface. Concepts and Thermodynamics. In *Calorimetry and Thermal Methods in Catalysis*; Auroux, A., Ed.; Springer Berlin Heidelberg: Berlin, 2013; Vol. *154*, pp 3−50.

DOI: 10.1021/acs.jpcc.6b03333
J. Phys. Chem. C 2016, 120, 12068−12074

(16) Ethiraj, J.; Albanese, E.; Civalleri, B.; Vitillo, J. G.; Bonino, F.; Chavan, S.; Shearer, G. C.; Lillerud, K. P.; Bordiga, S. Carbon Dioxide Adsorption in Amine-Functionalized Mixed-Ligand Metal-Organic Frameworks of Uio-66 Topology. *ChemSusChem* **2014**, *7*, 3382−3388.
(17) Grajciar, L.; Wiersum, A. D.; Llewellyn, P. L.; Chang, J. S.; Nachtigall, P. Understanding CO_2 Adsorption in CuBTC MOF: Comparing Combined DFT-Ab Initio Calculations with Microcalorimetry Experiments. *J. Phys. Chem. C* **2011**, *115*, 17925−17933.
(18) Llewellyn, P. L.; Bourrelly, S.; Serre, C.; Vimont, A.; Daturi, M.; Hamon, L.; De Weireld, G.; Chang, J. S.; Hong, D. Y.; Hwang, Y. K.; et al. High Uptakes of CO_2 and CH_4 in Mesoporous Metal-Organic Frameworks MIL-100 and MIL-101. *Langmuir* **2008**, *24*, 7245−7250.
(19) Bernini, M. C.; Blanco, A. A. G.; Villarroel-Rocha, J.; Fairen-Jimenez, D.; Sapag, K.; Ramirez-Pastor, A. J.; Narda, G. E. Tuning the Target Composition of Amine-Grafted CPO-27-Mg for Capture of CO_2 under Post-Combustion and Air Filtering Conditions: A Combined Experimental and Computational Study. *Dalton Trans.* **2015**, *44*, 18970−18982.
(20) Sprang, T.; Boddenberg, B. Coadsorption of Xenon and Carbon-Monoxide in Cadmium-Exchanged Zeolite-Y Studied with Xe-129 Nmr-Spectroscopy. *J. Chem. Soc., Faraday Trans.* **1995**, *91*, 555−558.
(21) Koch, M.; Brunner, E.; Pfeifer, H.; Zscherpel, D. Low-Temperature C-13 NMR Investigations on Carbon-Monoxide Hydrogen-Bonded to Bronsted Acid Sites in H-Y Zeolites. *Chem. Phys. Lett.* **1994**, *228*, 501−505.
(22) Klein, N.; Herzog, C.; Sabo, M.; Senkovska, I.; Getzschmann, J.; Paasch, S.; Lohe, M. R.; Brunner, E.; Kaskel, S. Monitoring Adsorption-Induced Switching by Xe-129 NMR Spectroscopy in a New Metal-Organic Framework Ni_2(2,6-ndc)$_2$(dabco). *Phys. Chem. Chem. Phys.* **2010**, *12*, 11778−11784.
(23) Hoffmann, H. C.; Assfour, B.; Epperlein, F.; Klein, N.; Paasch, S.; Senkovska, I.; Kaskel, S.; Seifert, G.; Brunner, E. High-Pressure in Situ Xe-129 NMR Spectroscopy and Computer Simulations of Breathing Transitions in the Metal-Organic Framework Ni_2(2,6-ndc)$_2$(dabco) (Dut-8(Ni)). *J. Am. Chem. Soc.* **2011**, *133*, 8681−8690.
(24) Kong, X. Q.; Scott, E.; Ding, W.; Mason, J. A.; Long, J. R.; Reimer, J. A. CO_2 Dynamics in a Metal-Organic Framework with Open Metal Sites. *J. Am. Chem. Soc.* **2012**, *134*, 14341−14344.
(25) Gul-E-Noor, F.; Mendt, M.; Michel, D.; Poppl, A.; Krautscheid, H.; Haase, J.; Bertmer, M. Adsorption of Small Molecules on Cu_3(Btc)$_2$ and Cu_3-Xzn$_x$(Btc)$_2$ Metal-Organic Frameworks (MOF) as Studied by Solid-State NMR. *J. Phys. Chem. C* **2013**, *117*, 7703−7712.
(26) Zukal, A.; Pawlesa, J.; Cejka, J. Isosteric Heats of Adsorption of Carbon Dioxide on Zeolite MCM-22 Modified by Alkali Metal Cations. *Adsorption* **2009**, *15*, 264−270.
(27) Caskey, S. R.; Wong-Foy, A. G.; Matzger, A. J. Dramatic Tuning of Carbon Dioxide Uptake Via Metal Substitution in a Coordination Polymer with Cylindrical Pores. *J. Am. Chem. Soc.* **2008**, *130*, 10870−10871.
(28) Dietzel, P. D. C.; Johnsen, R. E.; Fjellvag, H.; Bordiga, S.; Groppo, E.; Chavan, S.; Blom, R. Adsorption Properties and Structure of CO_2 Adsorbed on Open Coordination Sites of Metal-Organic Framework Ni_2(dhtp) from Gas Adsorption, IR Spectroscopy and X-Ray Diffraction. *Chem. Commun.* **2008**, 5125−5127.
(29) Sumida, K.; Stuck, D.; Mino, L.; Chai, J. D.; Bloch, E. D.; Zavorotynska, O.; Murray, L. J.; Dinca, M.; Chavan, S.; Bordiga, S.; et al. Impact of Metal and Anion Substitutions on the Hydrogen Storage Properties of M-BTT Metal-Organic Frameworks. *J. Am. Chem. Soc.* **2013**, *135*, 1083−1091.
(30) Kazansky, V. B. Drift Spectra of Adsorbed Dihydrogen as a Molecular Probe for Alkaline Metal Ions in Faujasites. *J. Mol. Catal. A: Chem.* **1999**, *141*, 83−94.
(31) Lamberti, C.; Zecchina, A.; Groppo, E.; Bordiga, S. Probing the Surfaces of Heterogeneous Catalysts by in Situ IR Spectroscopy. *Chem. Soc. Rev.* **2010**, *39*, 4951−5001.
(32) Breck, W. D. *Zeolite Molecular Sieves*; John Wiley & Sons, Inc.: New York, 1974.
(33) Arean, C. O.; Palomino, G. T.; Garrone, E.; Nachtigallova, D.; Nachtigall, P. Combined Theoretical and FTIR Spectroscopic Studies on Hydrogen Adsorption on the Zeolites Na-FER and K-FER. *J. Phys. Chem. B* **2006**, *110*, 395−402.
(34) Arean, C. O.; Delgado, M. R.; Palomino, G. T.; Rubio, M. T.; Tsyganenko, N. M.; Tsyganenko, A. A.; Garrone, E. Thermodynamic Studies on Hydrogen Adsorption on the Zeolites Na-ZSM-5 and K-ZSM-5. *Microporous Mesoporous Mater.* **2005**, *80*, 247−252.
(35) Zecchina, A.; Bordiga, S.; Vitillo, J. G.; Ricchiardi, G.; Lamberti, C.; Spoto, G.; Bjorgen, M.; Lillerud, K. P. Liquid Hydrogen in Protonic Chabazite. *J. Am. Chem. Soc.* **2005**, *127*, 6361−6366.
(36) Vedeneyev, V. I.; Gurvich, L. V.; Kondrat'yev, V. N.; Medvedev, V. A.; Frankevich, Y. L. *Bond Energies, Ionization Potentials and Electron Affinities*; St. Martins's Press: New York, 1962.
(37) Herzberg, G.; Monfils, A. The Dissociation Energies of H_2, HD and D_2 Molecules. *J. Mol. Spectrosc.* **1961**, *5*, 482.
(38) Zecchina, A.; Arean, C. O.; Palomino, G. T.; Geobaldo, F.; Lamberti, C.; Spoto, G.; Bordiga, S. The Vibrational Spectroscopy of H_2, N_2, CO and NO Adsorbed on the Titanosilicate Molecular Sieve Ets-10. *Phys. Chem. Chem. Phys.* **1999**, *1*, 1649−1657.
(39) Arean, C. O.; Tsyganenko, A. A.; Platero, E. E.; Garrone, E.; Zecchina, A. Two Coordination Modes of CO in Zeolites: A Temperature-Dependent Equilibrium. *Angew. Chem., Int. Ed.* **1998**, *37*, 3161−3163.
(40) Zecchina, A.; Bordiga, S.; Lamberti, C.; Spoto, G.; Carnelli, L.; Arean, C. O. Low-Temperature Fourier-Transform Infrared Study of the Interaction of CO with Cations in Alkali-Metal Exchanged ZSM-5 Zeolites. *J. Phys. Chem.* **1994**, *98*, 9577−9582.
(41) Vimont, A.; Thibault-Starzyk, F.; Daturi, M. Analysing and Understanding the Active Site by IR Spectroscopy. *Chem. Soc. Rev.* **2010**, *39*, 4928−4950.
(42) Valenzano, L.; Civalleri, B.; Chavan, S.; Palomino, G. T.; Arean, C. O.; Bordiga, S. Computational and Experimental Studies on the Adsorption of CO, N_2, and CO_2 on Mg-MOF-74. *J. Phys. Chem. C* **2010**, *114*, 11185−11191.
(43) Cavka, J. H.; Jakobsen, S.; Olsbye, U.; Guillou, N.; Lamberti, C.; Bordiga, S.; Lillerud, K. P. A New Zirconium Inorganic Building Brick Forming Metal Organic Frameworks with Exceptional Stability. *J. Am. Chem. Soc.* **2008**, *130*, 13850−13851.
(44) Bordiga, S.; Regli, L.; Bonino, F.; Groppo, E.; Lamberti, C.; Xiao, B.; Wheatley, P. S.; Morris, R. E.; Zecchina, A. Adsorption Properties of HKUST-1 toward Hydrogen and Other Small Molecules Monitored by IR. *Phys. Chem. Chem. Phys.* **2007**, *9*, 2676−2685.
(45) Arean, C. O.; Delgado, M. R.; Frolich, K.; Bulanek, R.; Pulido, A.; Bibiloni, G. F.; Nachtigall, P. Computational and Fourier Transform Infrared Spectroscopic Studies on Carbon Monoxide Adsorption on the Zeolites Na-ZSM-5 and K-ZSM-5: Evidence of Dual-Cation Sites. *J. Phys. Chem. C* **2008**, *112*, 4658−4666.
(46) Garrone, E.; Bulanek, R.; Frolich, K.; Arean, C. O.; Delgado, M. R.; Palomino, G. T.; Nachtigallova, D.; Nachtigall, P. Single and Dual Cation Sites in Zeolites: Theoretical Calculations and FTIR Spectroscopic Studies on CO Adsorption on K-FER. *J. Phys. Chem. B* **2006**, *110*, 22542−22550.
(47) Nachtigall, P.; Delgado, M. R.; Frolich, K.; Bulanek, R.; Palomino, G. T.; Bauca, C. L.; Arean, C. O. Periodic Density Functional and FTIR Spectroscopic Studies on CO Adsorption on the Zeolite Na-FER. *Microporous Mesoporous Mater.* **2007**, *106*, 162−173.
(48) Nachtigall, P.; Delgado, M. R.; Nachtigallova, D.; Arean, C. O. The Nature of Cationic Adsorption Sites in Alkaline Zeolites-Single, Dual and Multiple Cation Sites. *Phys. Chem. Chem. Phys.* **2012**, *14*, 1552−1569.

DOI: 10.1021/acs.jpcc.6b03333
J. Phys. Chem. C 2016, 120, 12068−12074